Supporting Information

On the Sensitivity of Folding Molecular Dynamics Simulations to Even Minor Force Field Changes.

Athanasia-Panagiota Serafeim, Georgios Salamanos,
Kalliopi K. Patapati and Nicholas M. Glykos

Department of Molecular Biology and Genetics,
Democritus University
of Thrace, University campus, 68100
Alexandroupolis, Greece, Tel +30-25510-30620,
Fax +30-25510-30620, http://utopia.duth.gr/glykos/ ,
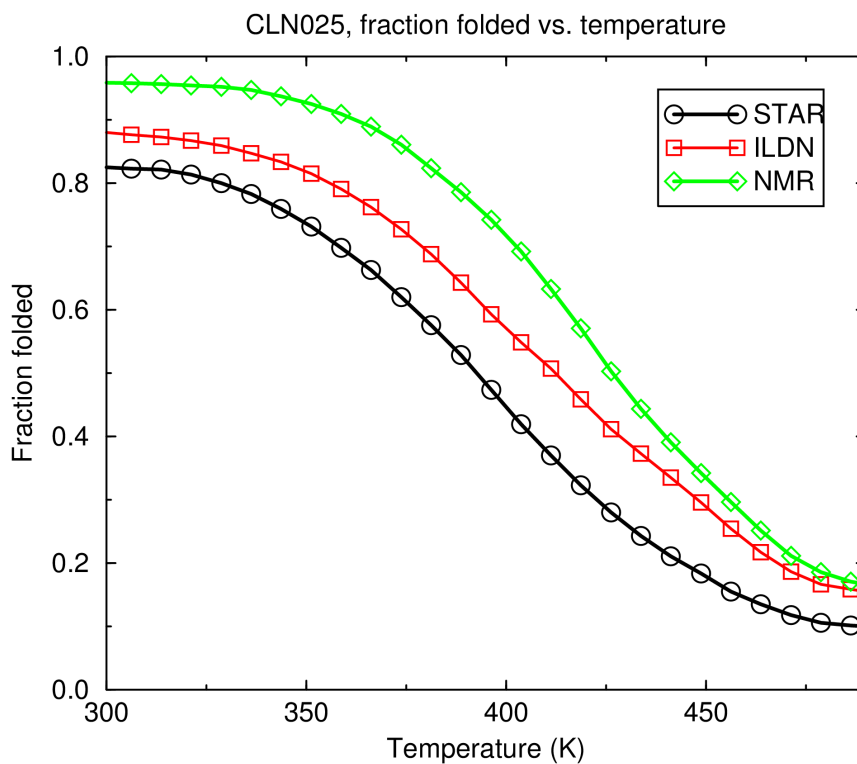glykos@mbg.duth.gr

Figure S1

Figure S1 : CLN025, Fraction of folded structures vs. Temperature. The three graphs in this diagram depict the variation of the fraction of folded structures as a function of temperature for each of the three force fields studied. Folded structures were classified as those having similarity Q values (with respect to the experimental NMR structure) greater than 0.55 (see the Q-T diagrams of Fig.2 of the main paper).
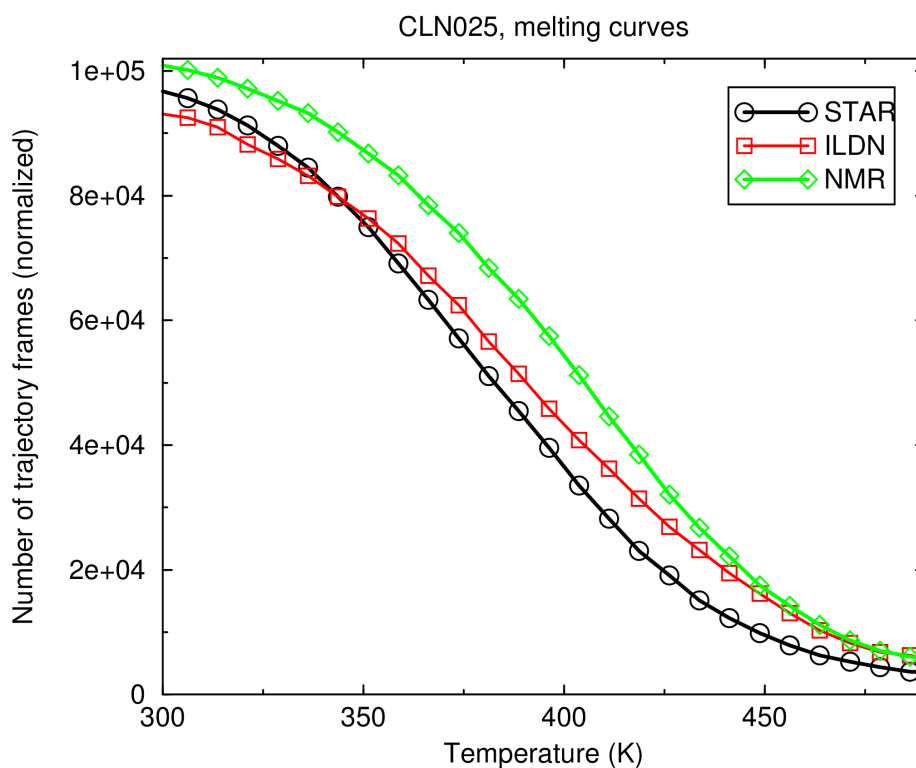
Figure S2

Figure S2 : CLN025, melting curves of the native structure. The three graphs in this diagram compare the melting curves of the native (β-hairpin) structure as a function of temperature for the three force fields studied. The graphs correspond to vertical –that is, constant Q– sections of the Q-T diagrams (Fig.2 of the main paper) taken at the Q values that maximized the folded population of the respective force fields. The vertical axis in this graph is proportional to the population of structures expressed as number of frames from the corresponding trajectories (the number of frames has been normalized to correct for the unequal sampling of different temperatures due to adaptive tempering).

Figure S3

HN chemical shifts
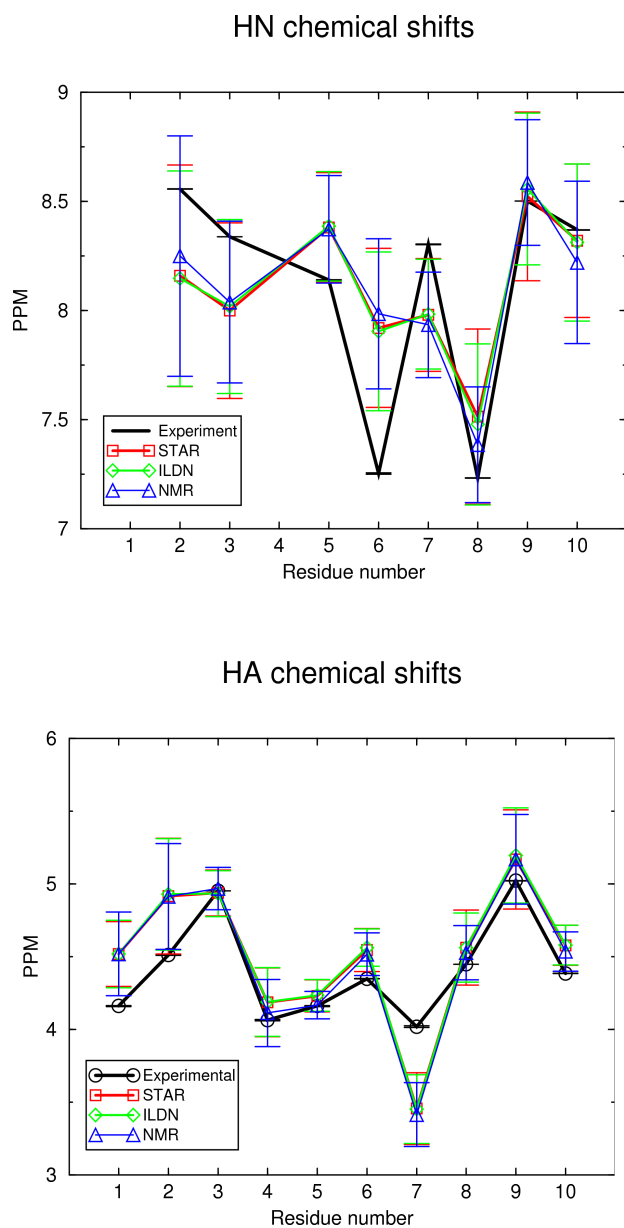

HA chemical shifts

Figure S3 : CLN025, chemical shifts, experimental vs. simulation derived. The two graphs in this diagram compare the experimental (thick black lines) with the simulation derived (red, green, blue lines) for the HN and HA chemical shifts. Error bars denote the 1σ level.
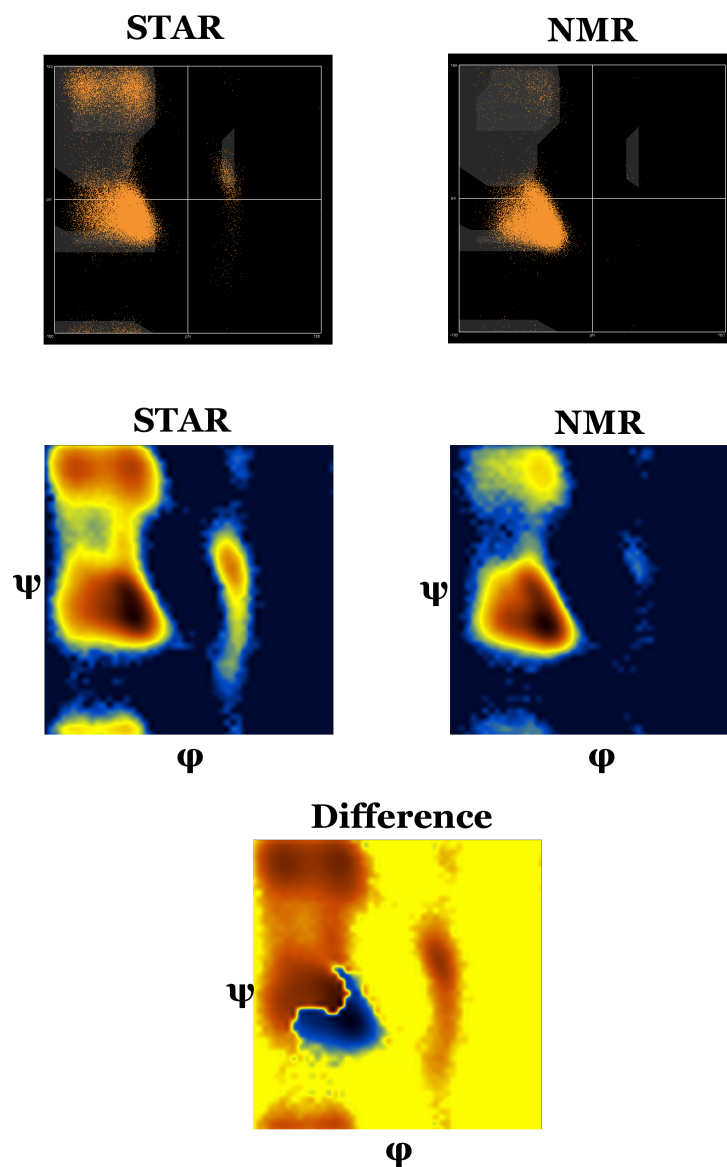
Figure S4

Figure S4 : αLa peptide, Ramachandran and difference Ramachandran plots. The two graphs in the top row show the cumulative Ramachandran plots for residues 3-7 as obtained from the whole of the STAR and NMR simulations. The middle two graphs show the corresponding log density distributions (with hot colors indicating large number of corresponding structures). The lower graph is the difference map between the Ramachandran plots of the form (STAR minus NMR). Positive values (higher density for STAR) is shown with warm colors, negative values (higher density for NMR) is depicted with cold colors. All graphs on the same scale.

Table S1

CLN025 : experimental vs MD-derived NOEs and their estimated standard deviations

Proton Indices	NOE (EXP)	NOE (STAR)	σ (STAR)	NOE (ILDN)	σ (ILDN)	NOE (NMR)	σ (NMR)
122-126	3.75	2.611263	0.538095	2.589342	0.494052	2.534155	0.314964
126-146	4.66	3.597264	0.556447	3.685342	0.510994	4.020951	0.316087
108-112	3.61	2.781489	0.484556	2.771055	0.472551	2.742704	0.443714
127-130	3.82	2.93632	0.580237	2.923893	0.577842	2.889541	0.569727
126-130	3.82	3.125396	0.54962	3.143341	0.545991	3.189156	0.534267
108-114	4.51	4.214299	0.544288	4.244267	0.528531	4.358816	0.478145
93-101	4.75	5.064103	0.423772	5.08835	0.415293	5.102678	0.412836
114-146	4.82	5.875258	1.170809	5.824237	1.164016	5.582342	1.154325
30-46	4.82	4.019499	0.273389	4.05379	0.241924	4.034287	0.264627
29-46	4.82	4.02309	0.26051	4.02234	0.269612	4.064283	0.238731
46-50	3.56	3.036333	0.28654	3.009743	0.268291	2.990794	0.236223
46-51	3.56	2.557921	0.257028	2.536876	0.232684	2.512684	0.197046
59-72	3.66	2.980893	0.386405	2.974821	0.379217	2.968205	0.344784
33-65	4.26	6.469092	1.647051	6.483796	1.582267	6.603936	1.556512
33-132	5.02	5.032921	2.489723	4.941119	2.527135	4.716088	2.421841
35-132	4.68	5.288005	2.774603	5.148759	2.871302	4.998808	2.783247
35-139	5.50	5.944403	2.796608	5.862881	2.656843	5.549402	2.272082
6-12	3.81	3.284419	0.819923	3.295452	0.816888	3.504374	0.721132
112-156	4.39	3.63943	2.489036	3.526713	2.257834	3.356214	2.140418
114-156	4.66	4.371134	2.537939	4.282522	2.233512	4.244754	2.160627
27-35	4.51	5.339021	0.599355	5.306223	0.607211	5.232895	0.615931
146-163	3.74	3.591461	1.000734	3.662933	1.004141	3.518086	1.036651
122-130	4.74	3.502382	1.084235	3.550816	1.072898	3.618254	1.065333
101-108	3.44	2.687964	0.701233	2.663091	0.632297	2.663896	0.351343
122-141	5.37	3.365842	1.317315	3.354144	1.321774	3.346444	1.339449
87-101	2.82	2.16851	0.310808	2.156553	0.329216	2.299892	0.29949
72-87	3.29	2.483315	0.301629	2.483952	0.287789	2.66302	0.267832
46-154	4.97	4.838374	2.594991	4.564385	2.664167	4.506604	2.266764

40-46	4.37	4.736105	0.779407	4.770073	0.748001	4.833017	0.739288
122-127	3.75	3.189703	0.463282	3.142397	0.487015	3.1216	0.508849
127-146	4.66	3.146561	0.578307	3.151062	0.568785	3.211784	0.545467
112-122	4.16	3.499187	0.590874	3.521502	0.580679	3.544805	0.566839
112-146	5.02	5.928225	0.589784	5.949238	0.588982	5.770388	0.544264
110-146	5.50	5.964486	0.502432	6.034735	0.427114	6.016305	0.362318
27-46	3.13	2.207062	0.172952	2.198623	0.147315	2.19668	0.151263
110-122	2.94	2.230195	0.292339	2.215435	0.220633	2.213718	0.228635
33-62	4.85	5.825221	1.888518	5.874074	1.828302	5.704595	1.868715
35-65	3.22	5.315469	2.127923	5.339321	1.970031	5.598151	1.959192
27-124	4.10	2.59508	2.084526	2.545076	1.827179	2.47893	1.337663
87-93	4.06	3.542166	0.66625	3.530442	0.656217	3.335784	0.648174
114-122	4.14	3.294734	0.856329	3.280386	0.826915	3.216308	0.808561
6-19	4.74	5.454479	0.684971	5.435217	0.686303	5.695744	0.676185
148-154	3.64	3.285968	0.694244	3.344444	0.675751	3.282436	0.677179
148-156	5.50	5.336914	0.548913	5.377438	0.541925	5.303504	0.509195
14-48	3.96	4.863568	2.748349	4.657779	2.64969	4.696577	2.373711
12-48	4.32	5.787922	1.731603	5.643744	1.690827	5.293448	1.79898
124-141	3.93	3.706897	0.658395	3.688694	0.655497	3.622124	0.655022
124-130	4.55	3.582732	0.573457	3.569232	0.566882	3.52859	0.542416
35-62	5.21	5.63619	2.133514	5.705709	1.997492	5.669815	2.040834
33-68	3.76	4.781491	1.242232	4.784082	1.149071	4.794126	1.13406
35-68	4.78	3.316197	1.803932	3.351003	1.592067	3.348361	1.633349
33-59	5.01	5.46119	1.494116	5.496767	1.451313	5.546737	1.441237
35-124	4.41	6.032474	2.130528	5.910521	2.045829	5.689949	1.664222
27-163	5.50	4.402874	2.441918	4.486989	2.522242	4.453093	2.213683
112-154	4.93	5.180383	1.6504	5.003461	1.543339	4.876362	1.469618
91-108	4.87	4.137942	0.907928	4.101326	0.860539	4.071301	0.596155
124-163	4.94	4.179185	1.479934	4.273717	1.466191	4.270643	1.43551
35-141	4.82	5.706337	2.555284	5.567262	2.446804	5.356828	2.129189
35-130	3.98	5.881998	2.383553	5.744857	2.470663	5.571386	2.317395
33-141	4.45	4.571872	2.588202	4.423927	2.518171	4.190296	2.264338
74-79	4.00	2.806485	0.460675	2.797467	0.462702	2.884604	0.459471
48-59	3.25	2.343479	0.29979	2.331307	0.290712	2.372057	0.27804
19-50	4.73	3.767346	2.93328	3.760237	2.761316	3.663907	2.590303

25-29	3.68	3.077913	0.297201	3.079197	0.29583	2.979677	0.287676
29-59	4.42	7.201415	0.526587	7.173263	0.51028	7.132571	0.458847
29-141	4.53	3.715266	2.537746	3.640735	2.36437	3.434512	2.109242
29-139	4.27	4.157322	2.894416	4.100192	2.723361	3.862507	2.490748
33-126	5.04	4.879706	2.512838	4.698596	2.503227	4.421095	2.328356
46-50	3.10	3.036333	0.28654	3.009743	0.268291	2.990794	0.236223
50-72	4.62	4.582001	0.473684	4.657972	0.405883	4.741895	0.401063
50-91	4.52	5.629558	1.056132	5.792717	0.898546	6.164707	0.63425
50-108	3.61	4.729146	1.350505	4.64359	1.17846	4.523274	0.73378
50-112	4.33	4.501912	2.134667	4.398521	1.907666	4.327387	1.377877
50-154	4.66	4.607829	2.916911	4.331876	2.846053	4.175363	2.258976
50-156	3.76	3.717754	3.418357	3.501133	3.290203	3.423573	2.591413
122-126	3.04	2.611263	0.538095	2.589342	0.494052	2.534155	0.314964
126-130	3.33	3.125396	0.54962	3.143341	0.545991	3.189156	0.534267
126-141	3.44	3.028881	0.724638	3.011334	0.720955	2.972841	0.706843
126-146	4.03	3.597264	0.556447	3.685342	0.510994	4.020951	0.316087
146-150	3.54	2.675047	0.424641	2.676857	0.434719	2.575172	0.339306